Meccanica (2015) 50:2977–2994
DOI 10.1007/s11012-015-0172-6

Influence of corrugated boundary surfaces, reinforcement, hydrostatic stress, heterogeneity and anisotropy on Love-type wave propagation

Abhishek Kumar Singh · Amrita Das · Santan Kumar · Amares Chattopadhyay

Received: 30 October 2014 / Accepted: 24 March 2015 / Published online: 3 April 2015

Abstract It may not be enough to hold all the engineering problems by the supposition that material mediums are isotropic, homogeneous, without initial stress and have a planar boundary surface, as the concept cannot indulge many features of the continuum response which are of great significance. This motivates us to study the influence of corrugated boundary surfaces, reinforcement, hydrostatic stress, heterogeneity and anisotropy on the propagation of Love-type wave in a corrugated heterogeneous orthotropic layer lying over a fibre-reinforced half-space under hydrostatic state of stress. The heterogeneity in the upper corrugated layer is caused due to exponential variation in the elastic constants with respect to the space variable pointing positively downwards. The dispersion relation has been obtained in closed form and found in well-agreement to the classical Love wave equation. The substantial effect of corrugation parameters, reinforcement, undulatory parameter, hydrostatic state of stress, heterogeneity parameter, position parameter and wave number on the phase velocity of Love-type wave has been observed and depicted by means of graph. The comparative study to unravel the effect of presence and absence of corrugated boundary surfaces of layer, heterogeneity in upper layer, reinforcement in half-space and anisotropy existing in both layer and half-space, on the dispersion curve is among the important peculiarities of the present paper.

Keywords Corrugation · Dispersion · Orthotropic · Heterogeneity · Hydrostatic stress · Fibre-reinforced · Love-type wave

A. K. Singh · A. Das (✉) · S. Kumar · A. Chattopadhyay
Department of Applied Mathematics,
Indian School of Mines, Dhanbad 826004
Jharkhand, India
e-mail: amritadas.ism@gmail.com

1 Introduction

The study of longitudinal as well as shear wave (Love-type wave) velocity measurements find their worthy applications in a numerous geological and geophysical fields including water, oil, gas and other subsurface geological probing and exploration; and designing various civil engineering and marine structures such as dams, tunnels, highways, bridges, platforms, on-shore or off-shore structures and sub-surface development. The dispersion property of surface waves reveals that different wavelength has different penetration depth and hence it propagates with different velocity. The near-surface velocity profile could be analyzed with the aid of dispersion of surface waves, therefore makes the related study obligatory. In order to realize a high performance of the designs and construction quality, it is essential that the foundation bearing ground is rigorously investigated. Hence, the study of effect of

different affecting parameters of the medium on the shear wave velocity.

propagating through it may find applications in the arena of Geophysics and Geomechanics. For more evidences the papers including Singh et al. [1, 2] and may be referred where the considered problems is about the dispersion of Love-type wave (Shear wave) through different mediums.

The assumption that the constituent layers of earth are isotropic may not be adequate to encapsulate most of the engineering problems including response of soils, geological materials and composites. Moreover, it does not capture some considerable features of the continuum response. In spite of being a long uphill climb compared isotropic problems; the elasto-dynamic response of anisotropic problems has received the attention of several eminent researchers in the past years. Particularly, the problems concerning transversely isotropic and orthotropic materials have been more regularly studied.

Orthotropic materials are those in which the mechanical or thermal properties are unique and independent in three mutually perpendicular directions. Many fiber-reinforced composites, wood, cold-rolled steel, ceramics, as well as bone exemplify orthotropic materials. These materials have tremendous usage in engineering applications. According to Hooke's Law, orthotropic material involves nine material/elastic constants, whereas there are only two material constants for isotropic materials. Moreover, the composition of the earth is heterogeneous which indicates that a heterogeneous orthotropic/isotropic medium interfaces play a significant role in the propagation of seismic waves. Kumar and Kumar [3] investigated the effect of voids on the surface wave propagation in a layer of orthotropic thermoelastic material with voids lying over an isotropic elastic half-space. Kundu et al. [4] studied the propagation of shear waves (SH-type waves) in a homogeneous isotropic medium sandwiched between two semi-infinite media. The secular equation for surface acoustic waves propagating on an orthotropic incompressible half-space was derived by Destrade [5], in a direct manner using the method of first integrals. Chow [6] derived the dynamic equations of orthotropic laminated plates from the concepts of Timoshenko's beam theory to include the effects of transverse shear and rotatory inertia. The normalized change in ultrasonic natural velocity as a function of stress and temperature was measured and they were used together with the linear (second order) elastic moduli to calculate some of the nonlinear (third order) moduli of this material by Prosser and Green [7]. By using an appropriate representation of the solution, Vinh and Seriani [8] obtained the secular equation of the Stoneley wave in the explicit form. Moreover, considering its special cases, they derived explicit secular equations for a number of investigations of Stoneley waves under the influence of gravity, for which only the implicit dispersion equations were previously obtained. Kundu et al. [4] studied the influence of heterogeneity and initial stress on the dispersion of shear waves in a homogeneous isotropic medium sandwiched between two semi-infinite media.

There exist some materials which combine to form a new type of material. The properties of the newly formed composite are literally different from the individual materials, but the properties of the individual components remain aloof within the composite materials. An example of such composite material is the fibre-reinforced material. A fibre-reinforced material comprises of the fibre (dispersed phase), the matrix (continuous phase) and the interface between the ingredient materials. These fibre materials may be converted to self-reinforced fibres under certain temperature and pressure. Carbon, nylon or conceivable metal whiskers are some common examples of fibres. Fibre composites find its applications in the field of construction, aviation, space, geophysics and geomechanics. The technique of natural and synthetic fibre reinforcement of soils is a feasible technique for increasing a soil's strength and load-bearing capacity. Therefore, these techniques are used in large scale in a variety of applications ranging from retaining structures and embankments to subgrade stabilization beneath footings and pavements. The presence of self-reinforced materials in the earth crust, in the form of some hard/soft rocks, effects the propagation of seismic waves through them. The constitutive equations for a fibre-reinforced linearly anisotropic medium with respect to preferred direction were circumvented by Spencer [9]. Belfield et al. [10] gives the idea of introducing a continuous reinforcement at every point of an elastic solid. The propagation of magnetoelastic shear waves in an infinite self-reinforced plate was studied by Chattopadhyay and Choudhury [11]. A large amount of information related to Love wave propagation in fibre-reinforced

material with different geometries, could be gathered from the disquisitions of Chattopadhyay and Singh [12–14] and Chattopadhyay et al. [15, 16].

An isotropic stress that is given by the weight of water above a certain point is designated as hydrostatic stress. The hydrostatic stress, being an isotropic stress, acts equally in all directions. Hydrostatic stress (confining stress) finds its worthy applications in the arena of continuum mechanics, particularly in geomechanics and geophysics, where the initial stress is partially hydrostatic or the solid is found in contact with a fluid in hydrostatic equilibrium. The situation may arrive in case of compressible solids, incompressible solids and incompressible solid of uniform density submerged in a fluid of the same density. The solution to this may lead to a better practical insight of the geophysical problems. Although the hydrostatic stress does not have a much pronounced effect on incompressible solids, but its presence in the media through which a wave is propagating, coincide to real world scenario. The elasto-dynamical equations for transversely isotropic solids in order to investigate the general theory of transversely isotropic magneto-elastic interface waves in conducting media under initial hydrostatic tension or compression were employed by Acharya et al. [17]. Singh and Yadav [18] studied the reflection of plane waves at a free surface of a perfectly conducting transversely isotropic elastic solid half-space with initial stress.

A series of parallel ridges and furrows is termed as corrugation. The evidence for the presence of corrugated surfaces has been well-grounded by many researchers, keeping in view the natural structures (such as mountains, basins, mountain roots and salt and ore deposits present beneath earth etc.) as well as man-made structures (viz. the surface of various tanks, turbine bores, different wires, amusement park rides, tires etc.). The propagation of waves and vibrations through these structures gets affected by the undulation. Therefore, it is quite significant to study the effect of corrugated surfaces on the propagation of waves. Propagation and reflection/refraction of seismic waves through corrugated surface has been discussed by many researchers. Singh and Tomar [19] studied the qP-wave at a corrugated interface between two dissimilar pre-stressed elastic half-space using the Rayleigh's method of approximation. The study of reflection and transmission coefficients due to incident plane SH-waves at a corrugated interface between two isotropic, laterally and vertically heterogeneous viscoelastic solid half spaces were furnished by Kaur et al. [20]. Apart from these, Tomar and Kaur [21–23] had investigated on Reflection and transmission of SH-waves at a corrugated interface between (1) two laterally and vertically heterogeneous anisotropic elastic solid half-spaces (2) a dry sandy half-space and an anisotropic elastic half-space (3) two monoclinic solid half-spaces. Kundu et al. [24] briefly reported the existence of Love wave propagation in an initially stressed homogeneous layer over a porous half-space with irregular boundary surfaces. Singh [25] solved the problem of propagation of a Love wave in a corrugated isotropic layer over a homogeneous isotropic half-space. Using first-order perturbation theory of Whitham's equation for dispersive waves in non-uniform media, Ben-Hador and Buchen [26] derived the dispersion of Love and Rayleigh waves in multilayered models with smooth and weakly non-parallel boundaries. Singh et al. [27] obtained the expression for stresses produced due to a normal moving load on a rough monoclinic half-space and studied the effect of irregularity and heterogeneity on these stresses.

Even though a number of problems has been solved taking the phenomena of reflection/refraction of seismic waves in mediums with corrugated surfaces, but many problems regarding the propagation of seismic waves in corrugated medium are still unexplored.

The aim of the present paper is to characterize the influence of corrugated boundary surfaces, reinforcement, hydrostatic stress, heterogeneity and anisotropy, on the propagation of Love-type wave in a corrugated heterogeneous orthotropic layer lying over a fibre-reinforced half-space under hydrostatic state of stress. The heterogeneity in the layer is caused due to exponential variation in material constants with respect to the space variable pointing positively downwards. The dispersion relation has been obtained in closed form and found in assent with the classical Love wave equation as a particular case of the problem. The pronounced effect of corrugation parameters, reinforcement, undulatory parameter, hydrostatic state of stress, heterogeneity parameter, position parameter and wave number on phase velocity has also been studied numerically and demonstrated graphically.

2 Formulation of the problem

In the present context, we consider the propagation of Love-type wave in a corrugated heterogeneous orthotropic layer lying over a fibre reinforced half-space under hydrostatic state of stress, as shown in Fig. 1. The heterogeneity in the orthotropic layer is caused due to exponential variation of space variable which is pointing positively downwards. Cartesian co-ordinate system has been taken in such a way that origin, O is at the common interface of the layer and half-space, x-axis is along the direction of propagation of Love-type wave and z-axis is pointing vertically downward. The average width of the layer is H and the half-space lies in the region $0 < \infty$. The uppermost boundary surface of the layer is defined as $z = g_1(x) - H$, and the common interface of the layer and the half-space is given by $z = g_2(x)$, where $g_1(x)$ and $g_2(x)$ are continuous periodic functions of x and independent of y.

Taking a suitable origin of coordinates the Trigonometric Fourier series of $g_1(x)$ and $g_2(x)$ can be represented as follows (Asano [28]):

$$g_l = \sum_{n=1}^{\infty} \left[g_n^{(l)} e^{in\lambda x} + g_{-n}^{(l)} e^{-in\lambda x} \right], \quad l = 1, 2, \tag{1}$$

where $g_n^{(l)}$ and $g_{-n}^{(l)}$ are Fourier expansion coefficients and n is series expansion order. Let us introduce the constants $a, b, R_n^{(l)}, I_n^{(l)}$ as follows:

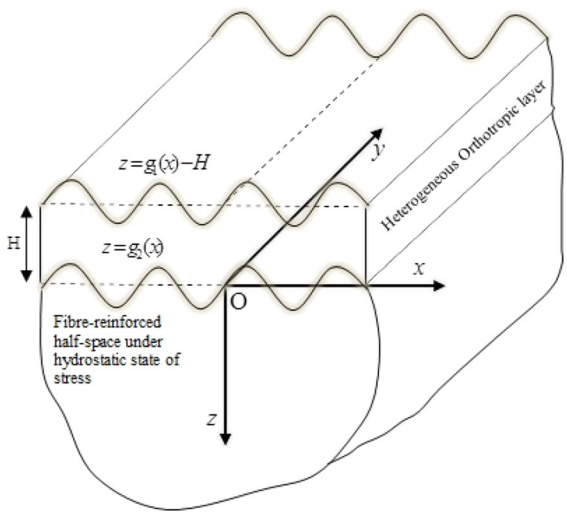

Fig. 1 Geometry of the problem

$$g_{\pm 1}^{(1)} = \frac{a}{2},\ g_{\pm 1}^{(2)} = \frac{b}{2},\ g_{\pm n}^{(l)} = \frac{R_n^{(l)} \mp I_n^{(l)}}{2},$$
$$l = 1, 2, \text{ and } n = 2, 3, \ldots$$

and

$$g_1 = a\cos\lambda x + R_2^{(1)}\cos 2\lambda x + I_2^{(1)}\sin 2\lambda x + \ldots + R_n^{(1)}\cos n\lambda x + I_n^{(1)}\sin n\lambda x + \ldots,$$

$$g_2 = b\cos\lambda x + R_2^{(2)}\cos 2\lambda x + I_2^{(2)}\sin 2\lambda x + \ldots + R_n^{(2)}\cos n\lambda x + I_n^{(2)}\sin n\lambda x + \ldots,$$

where $R_n^{(l)}, I_n^{(l)}$ are the cosine and sine Fourier coefficients, respectively. The upper and lower boundary surfaces of the layer in the concerned problem, may be expressed in terms of cosine i.e. $g_1 = a\cos\lambda x$ and $g_2 = b\cos\lambda x$, where λ is the wavenumber, a and b are the amplitudes of corrugation and the wavelength of corrugation is $2\pi/\lambda$.

Now, let u_i, v_i and $w_i (i = 1, 2)$ be the displacements along x, y and z directions respectively. For the propagation of Love-type wave in the x-direction causing displacement in y-direction only, we have

$$u_i = 0, v_i = v_i(x, z, t), w_i = 0. \tag{2}$$

2.1 Dynamics of the upper heterogeneous corrugated orthotropic layer and expression for displacement

The stress–strain relation for the upper heterogeneous orthotropic layer with y-being the diagonal axis is given by

$$\begin{bmatrix} \sigma_{11} \\ \sigma_{22} \\ \sigma_{33} \\ \sigma_{23} \\ \sigma_{13} \\ \sigma_{12} \end{bmatrix} = \begin{bmatrix} B_{11} & B_{12} & B_{13} & 0 & 0 & 0 \\ B_{12} & B_{22} & B_{23} & 0 & 0 & 0 \\ B_{13} & B_{23} & B_{33} & 0 & 0 & 0 \\ 0 & 0 & 0 & 2M & 0 & 0 \\ 0 & 0 & 0 & 0 & 2L & 0 \\ 0 & 0 & 0 & 0 & 0 & 2N \end{bmatrix} \begin{bmatrix} \varepsilon_{11} \\ \varepsilon_{22} \\ \varepsilon_{33} \\ \varepsilon_{23} \\ \varepsilon_{13} \\ \varepsilon_{12} \end{bmatrix}, \tag{3}$$

where σ_{ij} are the stress components, $B_{ij}(i, j = 1, 2, 3)$ and L, M, N are the elastic constants and ε_{ij} are the strain components.

Using Eq. (2), the strain–displacement relation for upper layer are obtained as

$$\varepsilon_{11} = 0, \varepsilon_{22} = 0, \varepsilon_{33} = 0, \varepsilon_{23} = \frac{1}{2}\frac{\partial v_1}{\partial z}, \varepsilon_{13} = 0,$$
$$\varepsilon_{12} = \frac{1}{2}\frac{\partial v_1}{\partial x}. \tag{4}$$

Using Eq. (4), the relations in Eq. (3) give

$$\sigma_{11} = \sigma_{22} = \sigma_{33} =, \sigma_{13} = 0, \sigma_{23} = M\frac{\partial v_1}{\partial z}, \sigma_{21} = N\frac{\partial v_1}{\partial x}. \tag{5}$$

In view of Eq. (5), the only non-vanishing equation we are left with is given by

$$\frac{\partial \sigma_{21}}{\partial x} + \frac{\partial \sigma_{23}}{\partial z} = \rho_1 \frac{\partial^2 v_1}{\partial t^2}, \tag{6}$$

where ρ_1 is the density of the upper heterogeneous corrugated orthotropic layer.

Now, the elastic constants of the corrugated heterogeneous orthotropic layer are assumed as exponentially varying functions of depth i.e.

$$M = M^* e^{\alpha(z+H)}, N = N^* e^{\alpha(z+H)}, \rho_1 = \rho_1^* e^{\alpha(z+H)},$$

where M^*, N^*, ρ_1^* are the values of M, N, ρ_1 at the uppermost free surface i.e. at $z = -H$ and α is the heterogeneity parameter.

Therefore, the equation of motion for the propagation of Love-type wave in upper corrugated heterogeneous orthotropic layer is given by

$$\frac{\partial^2 v_1}{\partial z^2} + \alpha\frac{\partial v_1}{\partial z} + \frac{N^*}{M^*}\frac{\partial^2 v_1}{\partial x^2} = \frac{1}{\beta_1^2}\frac{\partial^2 v_1}{\partial t^2}, \tag{7}$$

where $\beta_1^2 = \frac{M^*}{\rho_1^*}$.

Let $v_1(x, z, t) = V_1(z)e^{ik(x-ct)}$ be the solution of Eq. (7). Under this assumption Eq. (7) takes the form

$$\frac{d^2 V_1}{dz^2} + \alpha\frac{dV_1}{dz} + k^2\left(\frac{c^2}{\beta_1^2} - \frac{N^*}{M^*}\right)V_1 = 0. \tag{8}$$

Therefore, in view of Eq. (8), the expression for displacement in the upper layer is obtained as

$$v_1 = e^{-\frac{\alpha}{2}z}(A\cos p_1 z + B\sin p_1 z)e^{ik(x-ct)}, \tag{9}$$

where A and B are arbitrary constants and

$$p_1 = \frac{1}{2}\sqrt{4k^2\left(\frac{c^2}{\beta_1^2} - \frac{N^*}{M^*}\right) - \alpha^2}.$$

2.2 Dynamics of the lower fibre-reinforced half-space under hydrostatic state of stress and expression for displacement

The constitutive equation for a fibre-reinforced linearly elastic anisotropic medium with preferred direction $\vec{a}$ of reinforcement, is given by (Belfield et al. [10])

$$\begin{aligned}\left(\sigma_{ij}\right)_1 =& \lambda'(\varepsilon_{kk})_1\delta_{ij} + 2\mu_T(\varepsilon_{kk})_1 + \alpha'\left(a_k a_m(\varepsilon_{km})_1\delta_{ij}\right.\\ &+ a_i a_j(\varepsilon_{kk})_1\big) + 2(\mu_L - \mu_T)\left(a_i a_k\left(\varepsilon_{kj}\right)_1\right.\\ &\left.+ a_j a_k(\varepsilon_{ki})_1\right) + \beta' a_k a_m(\varepsilon_{km})_1 a_i a_j,\\ &i, j, k, m = 1, 2, 3.\end{aligned} \tag{10}$$

where $\left(\sigma_{ij}\right)_1$ are stress components, $\left(\varepsilon_{ij}\right)_1 = \frac{1}{2}\left(\frac{\partial u_i}{\partial x_j} + \frac{\partial u_j}{\partial x_i}\right)$ are components of infinitesimal strain, δ_{ij} is Kronecker delta, $\vec{a} = (a_1, a_2, a_3)$ is the preferred directions of reinforcement such that $a_1^2 + a_2^2 + a_3^2 = 1$. The vector $\vec{a}$ may be function of position. Indices take the values 1, 2, 3 and summation convention is employed. α', β' and $(\mu_L - \mu_T)$ are reinforcement parameters. μ_T can be identified as the shear modulus in transverse shear across the preferred direction, and μ_L as the shear modulus in longitudinal shear in the preferred direction. α', β' are specific stress components to take into account different layers for concrete part of the composite material, λ' is Lame's constant of elasticity.

The only non-vanishing equation of motion for the propagation of Love-type wave in the fibre-reinforced half-space under hydrostatic state of stress, as per Eqs. (2) and (10) is obtained as (Biot [29])

$$\frac{\partial(\sigma_{21})_1}{\partial x} + \frac{\partial(\sigma_{23})_1}{\partial z} - p_0\nabla^2 v_2 = \rho_2\frac{\partial^2 v_2}{\partial t^2}, \tag{11}$$

where p_0 is the hydrostatic stress and ρ_2 is the density of the fibre-reinforced half-space. Also, in Eq. (11) we have

$$\nabla^2 = \frac{\partial^2}{\partial x^2} + \frac{\partial^2}{\partial z^2}, \tag{12}$$

$$\left.\begin{aligned}(\sigma_{21})_1 &= \mu_T\frac{\partial v_2}{\partial x} + (\mu_L - \mu_T)a_1\left(a_1\frac{\partial v_2}{\partial x} + a_3\frac{\partial v_2}{\partial z}\right),\\ (\sigma_{23})_1 &= \mu_T\frac{\partial v_2}{\partial z} + (\mu_L - \mu_T)a_3\left(a_1\frac{\partial v_2}{\partial x} + a_3\frac{\partial v_2}{\partial z}\right).\end{aligned}\right\} \tag{13}$$

In view of Eqs. (12) and (13), Eq. (11) lead to

$$\left(P - \frac{p_0}{\mu_T}\right)\frac{\partial^2 v_2}{\partial z^2} + \left(Q - \frac{p_0}{\mu_T}\right)\frac{\partial^2 v_2}{\partial x^2} + R\frac{\partial^2 v_2}{\partial x \partial z} = \frac{1}{\beta_2^2}\frac{\partial^2 v_2}{\partial t^2}, \tag{14}$$

where,

$$P = 1 + \left(\frac{\mu_L}{\mu_T} - 1\right)a_3^2, Q = 1 + \left(\frac{\mu_L}{\mu_T} - 1\right)a_1^2,$$
$$R = 2a_1a_3\left(\frac{\mu_L}{\mu_T} - 1\right), \beta_2 = \sqrt{\frac{\mu_T}{\rho_2}}. \quad (15)$$

Now, we assume harmonic solution of the Eq. (14) of the form

$$v_2(x,z,t) = V_2(z)e^{ik(x-ct)}, \quad (16)$$

where k is the wave number and c is the common wave velocity. Equation (14) when substituted upon by Eq. (16), takes the form

$$\frac{d^2V_2}{dz^2} + \left(\frac{ikR}{P-p_0'}\right)\frac{dV_2}{dz} + k^2\left\{\frac{c^2/\beta_2^2 - (Q-p_0')}{P-p_0'}\right\} = 0, \quad (17)$$

where $p_0' = \frac{p_0}{\mu_T}$.

The solution of Eq. (17) gives the expression for displacement in lower fibre-reinforced half-space under hydrostatic state of stress as

$$v_2(x,z,t) = Ce^{-p_2z}e^{ik(x-ct)}, \quad (18)$$

where C is arbitrary constant and

$$p_2 = p_{re} + ip_{im},$$
$$p_{re} = \frac{k}{2}\sqrt{4\left(\frac{(Q-p_0') - c^2/\beta_2^2}{P-p_0'}\right) - \left(\frac{R}{P-p_0'}\right)^2},$$
$$p_{im} = \frac{1}{2}\left(\frac{Rk}{P-p_0'}\right).$$

3 Boundary conditions and dispersion relation

1. The uppermost corrugated surface of the layer is stress free i.e. at $z = g_1(x) - H$,

$$\sigma_{23} - g_1'\sigma_{12} = 0,$$

2. Stress is continuous at the common corrugated interface of layer and half-space i.e. at $z = g_2(x)$,

$$\sigma_{23} - g_2'\sigma_{12} = (\sigma_{23})_1 - g_2'(\sigma_{21})_1,$$

3. Displacement is continuous at the common corrugated interface of layer and half-space i.e. at $z = g_2(x)$,

$$v_1 = v_2,$$

where $g_1' = \frac{\partial g_1(x)}{\partial x}$ and $g_2' = \frac{\partial g_2(x)}{\partial x}$.

Using Eqs. (9) and (18) in boundary conditions (1), (2) and (3), we get

$$A = -B\frac{T_1\sin(p_1(g_1-H)) - T_2\cos(p_1(g_1-H))}{T_1\cos(p_1(g_1-H)) + T_2\sin(p_1(g_1-H))}, \quad (19)$$

$$C\mu_TT_4 = A[T_2\sin p_1g_2 + T_3\cos p_1g_2] + B[T_3\sin p_1g_2 + T_2\cos p_1g_2], \quad (20)$$

$$C = (A\cos p_1g_2 + B\sin p_1g_2)e^{-(\alpha/2-p_2)g_2}, \quad (21)$$

where

$$T_1 = g_1'N^*ik + \frac{\alpha}{2}M^*, T_2 = M^*p_1, T_3 = g_2'N^*ik + \frac{\alpha}{2}M^*,$$
$$T_4 = \left(R(ik + p_2g_2') - g_2'ikQ - Pp_2\right)e^{-(\alpha/2+p_2)g_2 - \alpha H}.$$

Eliminating the arbitrary constants from Eqs. (19), (20) and (21), we get

$$\tan[(g_2 - g_1 + H)p_1] = \frac{T_1T_2 + T_2T_4\mu_Te^{(p_2-\alpha/2)g_2} - T_2T_3}{T_2^2 - T_1T_4\mu_Te^{(p_2-\alpha/2)g_2} + T_1T_3}. \quad (22)$$

Equation (22) suggests that its right hand side is a complex expression. Therefore, equating the real and imaginary part gives

$$\tan[(g_2 - g_1 + H)p_1] = \frac{\psi_1\psi_2 + \psi_3\psi_4}{\psi_2^2 + \psi_4^2}, \quad (23)$$

where ψ_1, ψ_2, ψ_3 and ψ_4 are provided in "Appendix".

Equation (23), which comes from the comparison of real part on both the side, represents the dispersion equation for the Love-type wave propagating in a corrugated heterogeneous orthotropic layer lying over a fibre-reinforced half-space under hydrostatic state of stress.

4 Particular cases

Case 4.1 When $g_1 = 0$ and $g_2 = b\cos(\lambda x)$ i.e. the layer is bounded by an upper planar bounded surface and a lower corrugated boundary surface; the dispersion relation given in Eq. (23) takes the form

$$\tan[(b\cos\lambda x+H)p_1]=\frac{(\psi_1)_1(\psi_2)_1+(\psi_3)_1(\psi_4)_1}{(\psi_2)_1^2+(\psi_4)_1^2}. \tag{24}$$

Some special cases derived from Eq. (24) are as follows:

Subcase 4.1.1 When heterogeneity of the layer vanishes i.e. $\alpha=0$, Eq. (24) takes the form

$$\tan\left[(b\cos\lambda x+H)(p_1)_1\right]=\frac{p_{re}(P-Rb\lambda\sin\lambda x)}{M^*(p_1)_1},$$

which is the dispersion relation for the propagation of Love-type wave in a homogeneous orthotropic layer bounded by an upper planar surface and lower corrugated surface, lying over a fibre-reinforced half-space under hydrostatic state of stress.

Subcase 4.1.2 When the heterogeneity of layer and the hydrostatic stress acting in the half-space vanish i.e. $\alpha=0$ and $p_0'=0$, Eq. (24) becomes

$$\tan\left[(b\cos\lambda x+H)(p_1)_1\right]=\frac{(p_{re})_1(P-Rb\lambda\sin\lambda x)}{M^*(p_1)_1},$$

which is the dispersion relation for the propagation of Love-type wave in a homogeneous orthotropic layer bounded by an upper planar surface and lower corrugated surface, lying over a fibre-reinforced half-space under no hydrostatic state of stress.

Subcase 4.1.3 When the heterogeneity of layer and hydrostatic stress acting in the half-space vanish and the upper corrugated layer is isotropic i.e. $\alpha=0, p_0'=0, N^*=M^*=\mu_1$, Eq. (24) gives

$$\tan\left[(b\cos\lambda x+H)(p_1)_2\right]=\frac{(p_{re})_1(P-Rb\lambda\sin\lambda x)}{\mu_1(p_1)_2},$$

which is the dispersion relation for the propagation of Love-type wave in a homogeneous isotropic layer bounded by an upper planar surface and lower corrugated surface, lying over a fibre-reinforced half-space under no hydrostatic state of stress.

Subcase 4.1.4 When the layer and half-space are isotropic, heterogeneity of layer and hydrostatic stress acting in the half-space vanish and the lower corrugated boundary surfaces become planar, i.e. $\alpha=0,\ p_0'=0,\ N^*=M^*=\mu_1,\ a_1=0=a_3,\mu_L=\mu_T=\mu_2$ and $g_2=0$, Eq. (24) takes the form (Ewing et al. [30])

$$\tan\left[kH\sqrt{(c^2/\beta_1^2-1)}\right]=\frac{\mu_2\sqrt{(1-c^2/\beta_2^2)}}{\mu_1\sqrt{(c^2/\beta_1^2-1)}}, \tag{25}$$

which is the classical Love-wave equation.

Case 4.2 When $g_1=a\cos(\lambda x)$ and $g_2=0$ i.e. the layer is bounded by an upper corrugated surface and lower planar surface; the obtained dispersion relation given in Eq. (23) takes the form

$$\tan[(-a\cos\lambda x+H)p_1]=\frac{p_1p_{re}M^*Pe^{-\alpha H}(\psi_2)_2+M^*p_1\{kN^*g_1'+e^{-\alpha H}(kR+Pp_{im})\}(\psi_4)_2}{(\psi_2)_2^2+(\psi_4)_2^2}. \tag{26}$$

Some special cases derived from Eq. (26) are as follows:

Subcase 4.2.1 When heterogeneity of the layer vanishes i.e. $\alpha=0$, Eq. (26) takes the form

$$\tan\left[(-a\cos(\lambda x)+H)(p_1)_1\right]$$
$$=\frac{(p_1)_1p_{re}M^*P\left[\left\{(M^*)^2(p_1)_1^2+a\lambda\sin(\lambda x)N^*k(Rk+Pp_{im})\right\}-kN^*a\lambda\sin(\lambda x)_1(-kN^*a\lambda\sin(\lambda x)+kR+Pp_{im})\right]}{\left((M^*)^2(p_1)_1^2+a\lambda\sin(\lambda x)N^*k(Rk+Pp_{im})\right)^2+(-PkN^*p_{re}a\lambda\sin(\lambda x))^2},$$

which is the dispersion relation for the propagation of Love-type wave in a homogeneous orthotropic layer bounded by an upper corrugated surface and lower planar surface, lying over a fibre-reinforced half-space under hydrostatic state of stress.

Subcase 4.2.2 When the heterogeneity of layer and the hydrostatic stress acting in the half-space vanish i.e. $\alpha = 0$ and $p_0' = 0$, Eq. (26) becomes

$$\tan\left[(-a\cos\lambda x + H)(p_1)_1\right] = \frac{(p_1)_1(p_{re})_1 M^* P\left[\left\{(M^*)^2(p_1)_1^2 + a\lambda\sin(\lambda x)N^* k\left(Rk + P(p_{im})_1\right)\right\} - kN^* a\lambda\sin(\lambda x)_1\left(-kN^* a\lambda\sin(\lambda x) + kR + P(p_{im})_1\right)\right]}{\left((M^*)^2(p_1)_1^2 + a\lambda\sin(\lambda x)N^* k\left(Rk + P(p_{im})_1\right)\right)^2 + \left(-PkN^* a\lambda\sin(\lambda x)_1(p_{re})_1\right)^2},$$

which is the dispersion relation for the propagation of Love-type wave in a homogeneous orthotropic layer bounded by an upper corrugated surface and lower planar surface, lying over a fibre-reinforced half-space under no hydrostatic state of stress.

Subcase 4.2.3 When the heterogeneity of layer and hydrostatic stress acting in the half-space vanish and the upper corrugated layer is isotropic i.e. $\alpha = 0, p_0' = 0, N^* = M^* = \mu_1$, Eq. (26) gives

$$\tan\left[(-a\cos\lambda x + H)(p_1)_2\right] = \frac{(p_1)_2(p_{re})_1\mu_1^2 P\left[\left\{\mu_1(p_1)_2^2 + ka\lambda\sin(\lambda x)\left(Rk + P(p_{im})_1\right)\right\} - ka\lambda\sin(\lambda x)\left(-k\mu_1 a\lambda\sin(\lambda x) + kR + P(p_{im})_1\right)\right]}{\left(\mu_1^2(p_1)_2^2 + ka\lambda\sin(\lambda x)\left(Rk + P(p_{im})_1\right)\right)^2 + \left(-Pk\mu_1 a\lambda\sin(\lambda x)(p_{re})_1\right)^2},$$

which is the dispersion relation for the propagation of Love-type wave in a homogeneous isotropic layer bounded by an upper corrugated surface and lower planar surface, lying over a fibre-reinforced half-space under no hydrostatic state of stress.

Subcase 4.2.4 When the layer and half-space are isotropic, heterogeneity of layer and hydrostatic stress acting in the half-space vanish and the uppermost corrugated boundary surfaces become planar, i.e. $\alpha = 0$, $p_0' = 0$, $N^* = M^* = \mu_1$, $a_1 = 0 = a_3, \mu_L = \mu_T = \mu_2$ and $g_2 = 0$, Eq. (26) reduces to Eq. (25) which is the classical Love-wave equation (Ewing et al. [30]).

Case 4.3 When $g_1 = a\cos(\lambda x)$ and $g_2 = b\cos(\lambda x)$ i.e. the both the boundary surfaces of the layer are corrugated; the obtained dispersion relation given in Eq. (23) takes the form

$$\tan\left[((b-a)\cos(\lambda x) + H)p_1\right] = \frac{(\psi_1)_3(\psi_2)_3 + (\psi_3)_3(\psi_4)_3}{(\psi_2)_3^2 + (\psi_4)_3^2}, \tag{27}$$

Some special cases derived from Eq. (27) are as follows:

Subcase 4.3.1 When heterogeneity of the layer vanishes i.e. $\alpha = 0$, Eq. (27) takes the form

$$\tan\left[((b-a)\cos(\lambda x) + H)(p_1)_1\right] = \frac{(\psi_1)_4(\psi_2)_4 + (\psi_3)_4(\psi_4)_4}{(\psi_2)_4^2 + (\psi_4)_4^2},$$

which is the dispersion relation for the propagation of Love-type wave in a homogeneous orthotropic layer bounded by an upper and lower corrugated surfaces, lying over a fibre-reinforced half-space under hydrostatic state of stress.

Subcase 4.3.2 When the heterogeneity of layer and the hydrostatic stress acting in the half-space vanish i.e. $\alpha = 0$ and $p_0' = 0$, Eq. (27) becomes

$$\tan\left[((b-a)\cos(\lambda x)+H)(p_1)_1\right] = \frac{(\psi_1)_5(\psi_2)_5+(\psi_3)_5(\psi_4)_5}{(\psi_2)_5^2+(\psi_4)_5^2},$$

which is the dispersion relation for the propagation of Love-type wave in a homogeneous orthotropic layer bounded by an upper and lower corrugated surfaces, lying over a fibre-reinforced half-space under no hydrostatic state of stress.

Subcase 4.3.3 When the heterogeneity of layer and hydrostatic stress acting in the half-space vanish and the upper corrugated layer is isotropic i.e. $\alpha = 0, p_0' = 0, N^* = M^* = \mu_1$, Eq. (27) gives

$$\tan\left[((b-a)\cos(\lambda x)+H)(p_1)_2\right] = \frac{(\psi_1)_6(\psi_2)_6+(\psi_3)_6(\psi_4)_6}{(\psi_2)_6^2+(\psi_4)_6^2},$$

which is the dispersion relation for the propagation of Love-type wave in a homogeneous isotropic layer bounded by an upper and lower corrugated surfaces, lying over a fibre-reinforced half-space under no hydrostatic state of stress.

Subcase 4.3.4 When the layer and half-space are isotropic, heterogeneity of layer and hydrostatic stress acting in the half-space vanish and the boundary surfaces become planar instead of corrugated, i.e. $\alpha = 0,\ p_0' = 0,\ N^* = M^* = \mu_1,\ a_1 = 0 = a_3, \mu_L = \mu_T = \mu_2$ and $g_2 = 0$, Eq. (27) reduces to Eq. (25) which is the classical Love-wave equation (Ewing et al. [30]).

5 Numerical calculations and discussion

Numerical computations of the dispersion relation has been worked out with a purpose to emerge with the effect of corrugation parameter associated with upper and lower corrugated boundary surfaces of the layer, heterogeneity present in the layer, hydrostatic stress acting in the half-space and undulation parameter on the propagation of Love-type wave in a heterogeneous corrugated orthotropic layer overlying a fibre-reinforced half-space under hydrostatic stress.

The following data has been considered for computation purpose:

(a) For the upper corrugated heterogeneous orthotropic layer (Prosser and Green [7]):

$$M^* = 2.64\times10^9\,\mathrm{N/m^2},$$
$$N^* = 1.87\times10^9\,\mathrm{N/m^2} \text{ and } \rho_1 = 1442\,\mathrm{kg/m^3}.$$

(b) For the lower fibre-reinforced half-space under hydrostatic state of stress (Markham [31]):

$$\mu_L = 7.07\times10^9\,\mathrm{N/m^2},$$
$$\mu_T = 3.50\times10^9\,\mathrm{N/m^2} \text{ and } \rho_2 = 1600\,\mathrm{kg/m^3}.$$

In order to perform comparative study of the problem to the case when the Love-type wave is propagating in a corrugated heterogeneous isotropic layer lying over an isotropic half-space under hydrostatic state of stress, the following data has been considered (Gubbins [32]):

(a) For the upper corrugated heterogeneous isotropic layer:

$$\mu_1 = 32.3\times10^9\,\mathrm{N/m^2}, \rho_1 = 2802\,\mathrm{kg/m^3}.$$

(b) For the lower corrugated isotropic half-space under hydrostatic state of stress:

$$\mu_2 = 71.1\times10^9\,\mathrm{N/m^2}, \rho_2 = 2231\,\mathrm{kg/m^3}.$$

Moreover, the following data has been considered:

$$\alpha H = 0.1, 0.5, 0.9, p_0' = 0.1, 1.5, 2.0, 2.5,$$
$$\lambda H = 0.1, 0.15, 0.2, 1.4, kH = 2, a\lambda = 0.1, 0.2, 0.3,$$
$$b\lambda = 0.1, 0.2, 0.3, x/H = 0.05, 0.5, 0.15, 0.25,$$
$$a_1 = 0.00316227.$$

Figures 2–7 and 8 irradiates the effect of heterogeneity present in the layer, hydrostatic state of stress acting in the half-space, corrugation parameters associated with the upper and lower corrugated boundary surfaces of the layer, undulatory parameters and position parameter on the phase velocity of Love-type wave. Each of the figures consists of six curves in which curves 1, 2 and 3 corresponds to the case when a corrugated heterogeneous orthotropic layer lies over a

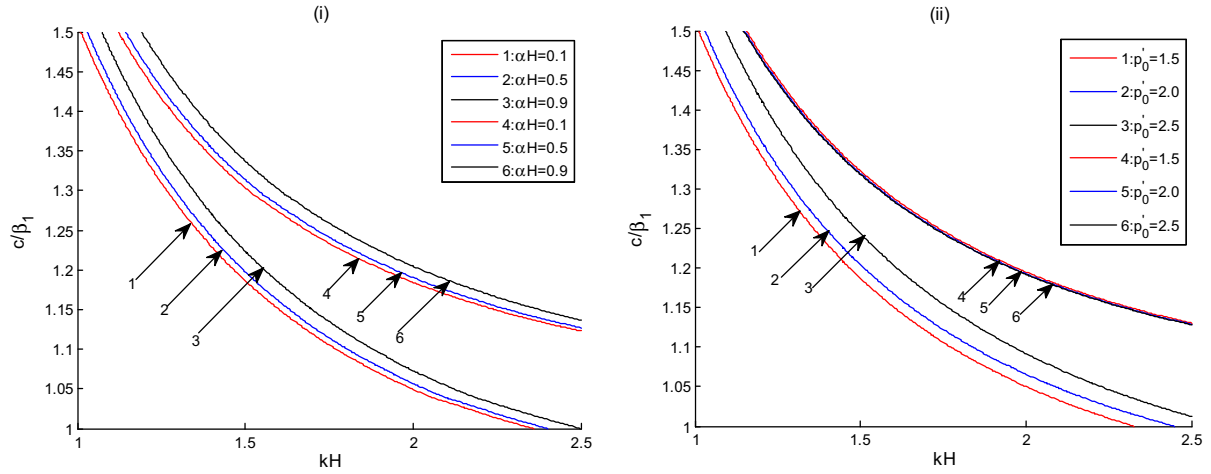

Fig. 2 Variation of phase velocity (c/β_1) against wave number (kH) **(i)** for different values of heterogeneity parameter (αH) of the layer when $p_0' = 0.1$ and; **(ii)** for different values of hydrostatic state of stress (p_0') when $\alpha H = 0.1$; for fixed $\lambda H = 1.4$, $a\lambda = 0.1$, $b\lambda = 0.1$, $x/H = 0.05$.

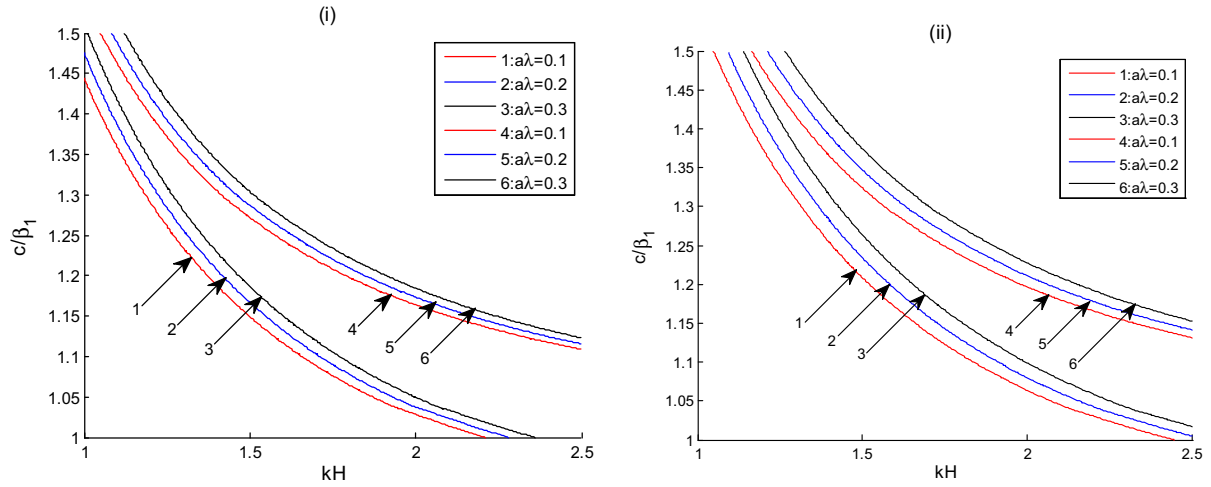

Fig. 3 Variation of phase velocity (c/β_1) against wave number (kH) **(i)** for different values of corrugation parameter of the upper boundary surface of layer $(a\lambda)$ when $b\lambda = 0.3$ (case 4.3); **(ii)** for different values of corrugation parameter of the upper boundary surface $(a\lambda)$ when $b\lambda = 0$ (case 4.2); for fixed $\lambda H = 1.4$, $\alpha H = 0.1$, $p_0' = 0.1$, $x/H = 0.05$.

fibre-reinforced half-space under hydrostatic state of stress and curves 4, 5 and 6 are associated to the case when corrugated heterogeneous isotropic layer lies over an isotropic reinforced-free half-space under hydrostatic state of stress.

Figures 2, 3, 4 and 5 shows the variation of phase velocity (c/β_1) against wave number (kH). These figures elucidate that phase velocity of Love-type wave decreases with increase in wave number. Figure 2(i), (ii) portrays the effect of variation of heterogeneity parameter of the layer and hydrostatic stress acting in the half-space respectively on phase velocity. It is clear from these figures that phase velocity of Love–type wave increases with increase in heterogeneity parameter as well as the hydrostatic state of stress in all anisotropic, isotropic, reinforced and reinforced-free cases. A minute observation of Fig. 2(i) elucidates that difference in phase velocity

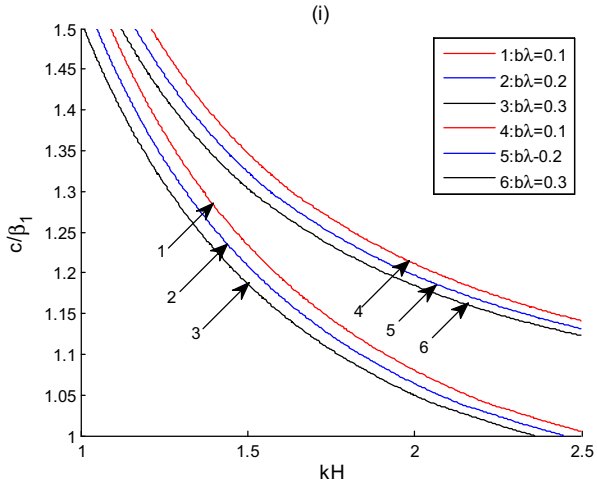

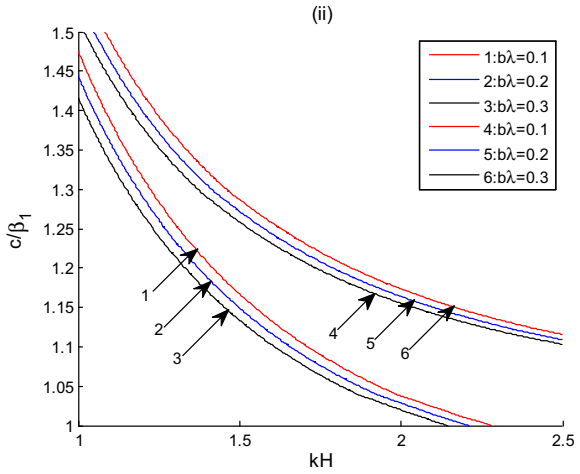

Fig. 4 Variation of phase velocity (c/β_1) against wave number (kH) (**i**) for different values of corrugation parameter of the lower boundary surface $(b\lambda)$ when $a\lambda = 0.3$ (case 4.3); (**ii**) for different values of corrugation parameter of the lower boundary surface $(b\lambda)$ when $a\lambda = 0$ (case 4.1); for fixed $\lambda H = 1.4$, $\alpha H = 0.1$, $p_0' = 0.1$, $x/H = 0.05$.

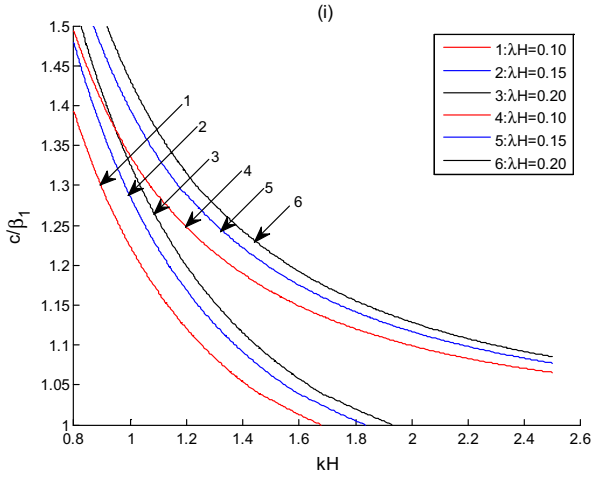

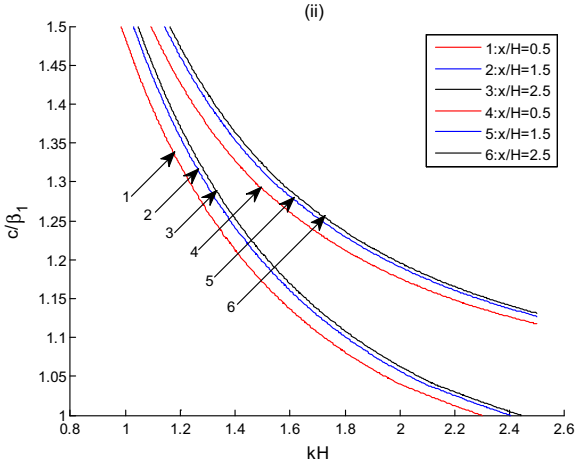

Fig. 5 Variation of phase velocity (c/β_1) against wave number (kH) (**i**) for different values of undulatory parameter (λH) when $x/H = 0.05$ (case 4.1); (**ii**) for different values of position parameter (x/H) when $\lambda H = 1.4$ (case 4.1); for fixed $\alpha H = 0.1$, $p_0' = 0.1$, $a\lambda = 0$, $b\lambda = 0.1$.

becomes more considerable with growing magnitude of heterogeneity for all anisotropic, isotropic, reinforced and reinforced-free cases. From Fig. 2(ii) it could be notified that for isotropic and reinforced-free case the influence of hydrostatic state of stress on phase velocity of Love-type wave is not significant.

Figure 3(i), (ii) illustrates the effect of corrugation parameter associated with the upper boundary surface of the layer $(a\lambda)$ on the phase velocity of Love-type wave when the common interface of the layer and half-space $(b\lambda)$ is considered corrugated and planar respectively. Curves plotted in Fig. 3(i) correspond to case 4.3 and curves plotted in Fig. 3(ii) correspond to case 4.2. These figures establish that phase velocity increases with increase in corrugation parameter associated with uppermost free surface of the layer

in all anisotropic, isotropic, reinforced and reinforced-free cases. Moreover, comparative study of the curves obtained in Fig. 3(i), (ii) establish that phase velocity in the presence of corrugation is more than the case of absence of corrugation in the common interface of layer and half-space. Apart from this, the effect of corrugation parameter associated with the upper boundary surface of layer is found more in the case when common interface of layer and half-space is planar as compared to the case when it is corrugated.

The effect of corrugation parameter associated with the common interface of the layer and half-space on phase velocity for the case when the corrugation parameter of the upper free boundary surface of the layer is corrugated and planar, has been manifested in Fig. 4(i), (ii) respectively. Figure 4(i) concurs to case 4.3 and Fig. 4(ii) corresponds to case 4.1. These figures suggest that phase velocity of Love-type wave decreases with increase in corrugation parameter associated with the common interface of the layer and half space in all anisotropic, isotropic, reinforced and reinforced-free cases. Comparative study of the curves in Fig. 4(i), (ii) establish that phase velocity in absence of corrugation is more than the case of presence of corrugation in upper boundary surface of layer. It has been found that the impact of corrugation parameter associated with common interface of layer and half space is more in the case when upper boundary surface is corrugated compared to the case when it is planar.

Curves plotted in Fig. 5(i), (ii) set forth the influence of undulatory parameter (λH) and position parameter (x/H) respectively on the phase velocity of Love-type wave. It could be notified from these figures that phase velocity increases with increase in undulatory parameter and position parameter in all anisotropic, isotropic, reinforced and reinforced-free cases. More interestingly, minute observation of Fig. 5(i) interprets that phase velocity of Love-type wave will be more if corrugated boundary surfaces of layer are steeply undulated and phase velocity of Love-type wave will be lesser if corrugated boundary surfaces of layer are modestly undulated in all anisotropic, isotropic, reinforced and reinforced-free cases. The undulatory parameter has pronounced effect on the phase velocity of Love-type wave. A small increase in the magnitude of undulatory parameter causes a significant increase in phase velocity. Unlike undulatory parameter, position parameter has considerably less effect on the phase velocity of Love-type wave. Figure 5(i), (ii) are associated with case 4.1.

The variation of phase velocity against corrugation parameter of the upper free boundary surface of the layer has been carved out in Fig. 6(i), (ii) for different values of corrugation parameter of lower boundary surface of layer and heterogeneity parameter of the layer respectively. Phase velocity is found to be decreasing with increase in corrugation parameter of the upper free boundary surface of the layer for particular value of corrugation parameter of the lower boundary surface of layer in all anisotropic, isotropic, reinforced and reinforced-free cases. Moreover, it has been observed in Fig. 6(i), (ii) that phase velocity increases with increase in corrugation parameter of the lower boundary surface of layer and heterogeneity parameter of the layer respectively. Figure 6(i) depictures that the percentage increase in phase velocity of Love-type wave for different values of corrugation parameter associated with the common interface of layer and half-space, is more immense in low frequency region as compare to high frequency region for all anisotropic, isotropic, reinforced and reinforced-free cases. A subtle and intense observation suggests that corrugation parameter of both upper and lower corrugated boundary surface of the layer have a substantial effect on the phase velocity but the effect of corrugation parameter of lower corrugated interface is much prominent.

Figure 7(i), (ii) shows the variation of phase velocity against corrugation parameter of the common interface of layer and half-space for different values of corrugation parameter of the upper free boundary surface of layer and heterogeneity parameter of layer respectively. These figures conclude that phase velocity of Love-type wave decreases with increase in corrugation parameter of the common interface of layer and half-space. Meticulous examination of Fig. 7(i) establishes that for all anisotropic, isotropic, reinforced and reinforced-free cases, at the beginning phase velocity increases with increase in corrugation parameter of the free surface but the curves invert their nature after a certain point, i.e. the phase velocity decreases with increase in corrugation parameter of the free surface after a certain fixed value of corrugation parameter of the common interface. Moreover, it is notified that the curves corresponding to the anisotropic and reinforced case are above the curves corresponding to isotropic and reinforced-free case at

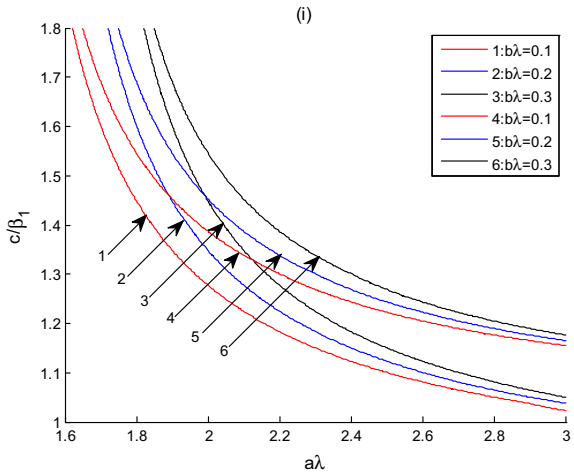

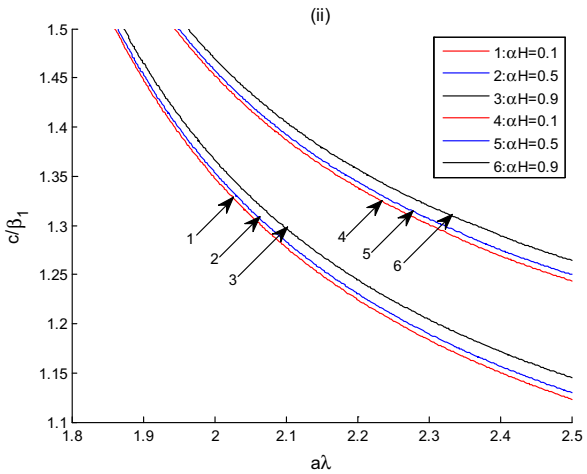

Fig. 6 Variation of phase velocity (c/β_1) against corrugation parameter of the upper boundary surface of layer $(a\lambda)$ (**i**) for different values of corrugation parameter of the lower boundary surface $(b\lambda)$ when $\alpha H = 0.1$ (**ii**) for different values of heterogeneity parameter of the layer (αH) when $b\lambda = 1.4$; for $p_0' = 0.1$, $\lambda H = 1.4$, $x/H = 0.05, kH = 2$.

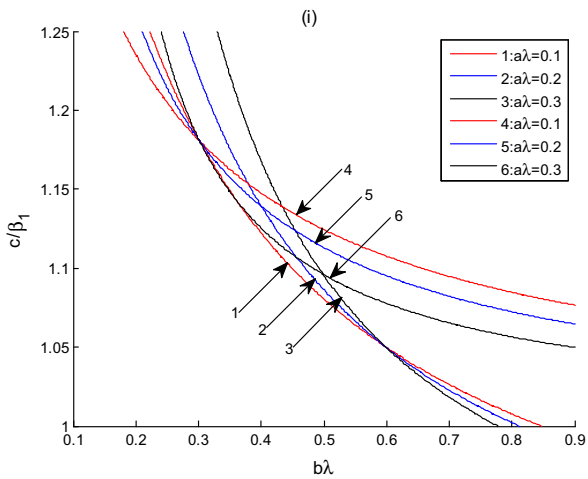

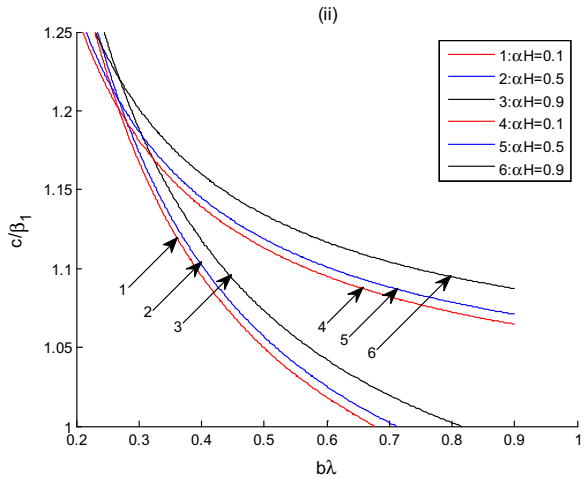

Fig. 7 Variation of phase velocity (c/β_1) against corrugation parameter of the lower boundary surface $(b\lambda)$ (**i**) for different values of corrugation parameter of the upper boundary surface of layer $(a\lambda)$ when $\alpha H = 0.1$; (**ii**) for different values of heterogeneity parameter of layer (αH) when $a\lambda = 0.1$; for fixed $p_0' = 0.1$, $\lambda H = 1.4$, $x/H = 0.05, kH = 2$.

the beginning, but after some time the behavior of the curves changes and curves corresponding to isotropic and reinforced-free case starts supporting more to the phase velocity of Love-type wave as compared to the curves corresponding to the anisotropic and reinforced case. The point (0.3, 1.18) is the point of inversion of the curves corresponding to isotropic and reinforced-free case; whereas the point (0.6, 1.051) is the point of inversion of the curves corresponding to anisotropic and reinforced case. Beside these, the co-ordinates (0.3, 1.18), (0.4, 1.14) and (0.5, 1.096) are the intersecting points where phase velocities corresponding to isotropic and reinforced-free case are same as the phase velocities corresponding to anisotropic and reinforced case for same values of corrugation parameter associated with the upper free boundary surface. In Fig. 7(ii), a monotonic increase in phase velocity of Love-type wave has been observed with

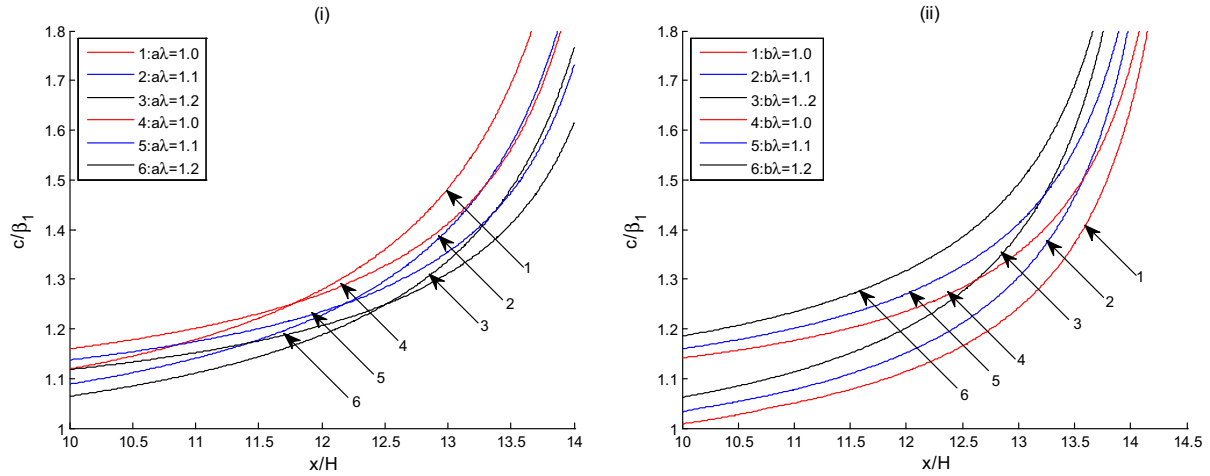

Fig. 8 Variation of phase velocity (c/β_1) against position parameter (x/H) (**i**) for different values of corrugation parameter of the upper boundary surface $(a\lambda)$ when $b\lambda = 0.1$; (**ii**) for different values of corrugation parameter of lower boundary surface $(b\lambda)$ when $a\lambda = 0.1$; for fixed $p_0' = 0.1$, $\lambda H = 1.4$, $\alpha H = 0.1, kH = 2$.

increase in heterogeneity parameter of the layer. The co-ordinates (0.2722, 1.204), (0.2677, 1.207) and (0.2679, 1.221) are the intersecting points where phase velocities corresponding to isotropic and reinforced-free case are same as the phase velocities corresponding to anisotropic and reinforced case for same values of heterogeneity parameter. More precisely Fig. 7(i), (ii) establish that in low frequency range phase velocity corresponding to isotropic and reinforced-free case is less than phase velocity corresponding to anisotropic and reinforced case for a particular value of heterogeneity parameter as well as corrugation parameter associated with the upper free boundary surface. Contrary to this, the trend gets reversed in high frequency range.

In Fig. 8(i), (ii), curves has been plotted in order to show the variation of phase velocity against position parameter for different values of corrugation parameter of the upper free boundary surface of layer and corrugation parameter of the common interface of layer and half-space respectively. Minute observation of curves plotted in Fig. 8(i) suggests that the curves corresponding to the anisotropic and reinforced case are below the curves corresponding to isotropic and reinforced-free case at the beginning, but after some time the scenario changes and the curves corresponding to anisotropic and reinforced case starts dominating curves corresponding to isotropic and reinforced-free case. The intersecting points after which the curves corresponding to anisotropic and reinforced case starts supporting more to phase velocity compared to isotropic and reinforced-free case are (11.77, 1.25), (12.18, 1.25) and (12.51, 1.25). Moreover, these co-ordinates represent that the three intersecting points possess a common phase velocity. Curves obtained in Fig. 8(ii) refers that there is an increase in phase velocity with increase in corrugation parameter of the common interface of layer and half-space. In both figures, the phase velocities corresponding to different values of corrugation parameters is found to be less in the region of low frequency whereas it is considerably high in the region of high frequency in all anisotropic, isotropic, reinforced and reinforced-free cases.

Comparative study of curves corresponding to isotropic case and anisotropic case reveals that dispersion curves associated with isotropic and reinforced-free case are lying above to the dispersion curves of anisotropic and reinforced case. Thus, it is observed that both anisotropy and reinforcement disfavors the phase velocity of Love-type wave. An average decrease of 10 % has been observed in the phase velocity of Love-type wave due to the presence of anisotropy and reinforcement in the medium. The percentage decrease in phase velocity is not uniform rather it increases with increase in wave number. Therefore, a conclusion can be drawn through an overview and comparative study of all the figures that as anisotropy

and reinforcement prevails in the medium, phase velocity of Love-type wave gets decreased.

6 Conclusions

The current study deals with the propagation of Love-type wave in a corrugated heterogeneous orthotropic layer overlying a fibre-reinforced half-space under hydrostatic state of stress. Closed form of the dispersion relation has been obtained. The dispersion relation is found to be significantly affected by the presence and absence of corrugation parameters of boundary surfaces of the layer, heterogeneity parameter of the layer and anisotropy present in both layer and half-space. Moreover, wavenumber, undulatory parameter and position parameter also have a pronounced effect on phase velocity of Love-type wave. Comparative study has been made to analyze the effect of these parameters on the curves corresponding to anisotropic, isotropic, reinforced and reinforced-free cases on the dispersion curves. The outcomes of the study are quoted as follows:

- The phase velocity of Love-type wave decreases with increase in the wave number in all anisotropic, isotropic, reinforced and reinforced-free cases.
- The corrugation parameter of the upper corrugated boundary surface of layer, hydrostatic stress, heterogeneity parameter, undulatory parameter and position parameter has a favouring effect on phase velocity in all anisotropic, isotropic, reinforced and reinforced-free cases, i.e. phase velocity increases with increase in the said parameters in all the cases.
- Phase velocity of Love-type wave has been found more in the case when corrugated boundary surfaces of layer are steeply undulated as compared to the case when corrugated boundary surfaces of layer are modestly undulated in all isotropic, anisotropic, reinforced and reinforced-free cases.
- Dispersion curves corresponding to isotropic and reinforced case is slightly affected by the variation of hydrostatic stress compare to the dispersion curves corresponding to isotropic and reinforced-free case.
- With increase in corrugation parameter of the common interface of the layer and half-space, the dispersion curve shifts downward in all isotropic, anisotropic, reinforced and reinforced-free cases, i.e. phase velocity decreases with increase in corrugation parameter of the interface in all the cases.
- In low frequency range phase velocity of Love-type wave is found less when isotropy prevails in the medium of layer and half-space compare to the anisotropy existing in the layer and half-space; but in high frequency range this trend alters.
- Presence of reinforcement in the medium of half-space favours the phase velocity of Love-type wave in low frequency range as compare to the case when reinforcement is absent in the medium of half-space, i.e. the reinforced-free half-space support less to the phase velocity in low frequency range. Contrary to this trend alters in high frequency region.
- In isotropic, homogeneous and reinforced-free case without hydrostatic state of stress, the dispersion relation of the problem matches with the classical Love-wave equation. This shows that the problem is in well agreement to the classical case (problem).

The current study may find its applications in the field of construction, retaining structures, embankments to subgrade stabilization beneath footings and pavements, aviation, space, geophysics and geomechanics because of the consideration of fibre-reinforced layer in it. The presence of self-reinforced materials in the earth crust, in the form of some hard/soft rocks, effects the propagation of seismic waves through them. Moreover, wood, cold-rolled steel, human bone, ceramics etc. are materials exhibiting orthotropic symmetry, which are very common to be found in nature. Hence, the present study is obligatory as the propagation of seismic waves through such media (reinforced and anisotropic) with corrugated boundary surfaces may be greatly affected by the characteristics.

Acknowledgments The authors convey their sincere thanks to Indian School of Mines, Dhanbad for providing JRF to Mr. Santan Kumar and Ms. Amrita Das and for facilitating them with its best facility.

Appendix

$$\psi_1 = p_1 p_{re} M^* \mu_T \left(R g_2' + P\right) e^{-\alpha(g_2+H)},$$

$$\begin{aligned}\psi_2 = {} & (M^*)^2 \left(\frac{\alpha^2}{4} + p_1^2\right) - g_1' g_2' k^2 (N^*)^2 \\ & + \mu_T e^{-\alpha(g_2+H)} \left\{ -g_1' N^* R k^2 + g_1' g_2' N^* Q k^2 \right. \\ & + \frac{\alpha}{2} M^* R p_{re} g_2' + \frac{\alpha}{2} M^* P p_{re} - g_1' g_2' N^* R k p_{im} \\ & \left. - g_1' N^* P k p_{im} \right\},\end{aligned}$$

$$\begin{aligned}\psi_3 = {} & M^* p_1 \left\{ k N^* \left(g_1' - g_2'\right) \right. \\ & \left. + e^{-\alpha(g_2+H)} \mu_T \left(k\left(R - Q g_2'\right) + p_{im}\left(R g_2' + P\right)\right) \right\},\end{aligned}$$

$$\begin{aligned}\psi_4 = {} & \frac{\alpha}{2} k M^* N^* \left(g_1' + g_2'\right) \\ & + e^{-\alpha(g_2+H)} \mu_T \left\{ \left(R g_2' + P\right) \left(k N^* g_1' p_{re} + \frac{\alpha}{2} M^* p_{im}\right) \right. \\ & \left. - \frac{\alpha}{2} k M^* \left(R - Q g_2'\right) \right\},\end{aligned}$$

$$(\psi_1)_1 = p_1 p_{re} M^* \mu_T (P - Rb\lambda \sin \lambda x) e^{-\alpha(b\cos \lambda x + H)},$$

$$\begin{aligned}(\psi_2)_1 = {} & (M^*)^2 \left(\frac{\alpha^2}{4} + p_1^2\right) \\ & + \mu_T e^{-\alpha(b\cos \lambda x + H)} \left\{ -\frac{\alpha}{2} M^* R p_{re} b\lambda \sin \lambda x \right. \\ & \left. + \frac{\alpha}{2} M^* P p_{re} \right\},\end{aligned}$$

$$\begin{aligned}(\psi_3)_1 = {} & M^* p_1 \left\{ k N^* b\lambda \sin \lambda x + e^{-\alpha(b\cos \lambda x + H)} \right. \\ & \left. \mu_T (k(R + Qb\lambda \sin \lambda x) + p_{im}(P - Rb\lambda \sin \lambda x)) \right\},\end{aligned}$$

$$\begin{aligned}(\psi_4)_1 = {} & -\frac{\alpha}{2} k M^* N^* b\lambda \sin \lambda x_2 \\ & + e^{-\alpha(b\cos \lambda x + H)} \mu_T \left\{ (P - Rb\lambda \sin \lambda x) \left(\frac{\alpha}{2} M^* p_{im}\right) \right. \\ & \left. - \frac{\alpha}{2} k M^* (R + Qb\lambda \sin \lambda x) \right\},\end{aligned}$$

$$\begin{aligned}(\psi_2)_2 = {} & (M^*)^2 \left(\frac{\alpha^2}{4} + p_1^2\right) \\ & + e^{-\alpha H} \mu_T \left\{ -g_1' N^* R k^2 + \frac{\alpha}{2} M^* P p_{re} \right. \\ & \left. - g_1' N^* P k p_{im} \right\},\end{aligned}$$

$$\begin{aligned}(\psi_4)_2 = {} & \frac{\alpha}{2} k M^* N^* g_1' \\ & + e^{-\alpha H} \mu_T \left\{ P \left(k N^* g_1' p_{re} + \frac{\alpha}{2} M^* p_{im}\right) \right. \\ & \left. - \frac{\alpha}{2} k M^* R \right\},\end{aligned}$$

$$(\psi_1)_3 = p_1 p_{re} M^* \mu_T (-Rb\lambda \sin(\lambda x) + P) e^{-\alpha(b\cos(\lambda x)+H)},$$

$$\begin{aligned}(\psi_2)_3 = {} & (M^*)^2 \left(\frac{\alpha^2}{4} + p_1^2\right) - ab\lambda^2 \sin^2(\lambda x) k^2 (N^*)^2 \\ & + \mu_T e^{-\alpha(b\cos(\lambda x)+H)} \left\{ a\lambda \sin(\lambda x) N^* R k^2 \right. \\ & + ab\lambda^2 \sin^2(\lambda x) N^* Q k^2 - \frac{\alpha}{2} M^* R p_{re} b\lambda \sin(\lambda x) \\ & + \frac{\alpha}{2} M^* P p_{re} - ab\lambda^2 \sin^2(\lambda x) N^* R k p_{im} \\ & \left. + a\lambda \sin(\lambda x) N^* P k p_{im} \right\},\end{aligned}$$

$$\begin{aligned}(\psi_3)_3 = {} & M^* p_1 \{ k N^* (b\lambda \sin(\lambda x) - a\lambda \sin(\lambda x)) \\ & + e^{-\alpha(b\cos(\lambda x)+H)} \mu_T (k(R + Qb\lambda \sin(\lambda x)) \\ & + p_{im}(-Rb\lambda \sin(\lambda x) + P)) \},\end{aligned}$$

$$\begin{aligned}(\psi_4)_3 = {} & -\frac{\alpha}{2} k M^* N^* (a\lambda \sin(\lambda x) + b\lambda \sin(\lambda x)) \\ & + e^{-\alpha(b\cos(\lambda x)+H)} \mu_T \{ (-Rb\lambda \sin(\lambda x) + P) \\ & \times \left(-k N^* a\lambda \sin(\lambda x) p_{re} + \frac{\alpha}{2} M^* p_{im}\right) \\ & \left. - \frac{\alpha}{2} k M^* (R + Qb\lambda \sin(\lambda x)) \right\},\end{aligned}$$

$$(\psi_1)_4 = (p_1)_1 p_{re} M^* \mu_T (-Rb\lambda \sin(\lambda x) + P),$$

$$\begin{aligned}(\psi_2)_4 = {} & (M^*)^2 (p_1)_1^2 - ab\lambda^2 \sin^2(\lambda x) k^2 (N^*)^2 \\ & + \mu_T \{ a\lambda \sin(\lambda x) N^* R k^2 \\ & + ab\lambda^2 \sin^2(\lambda x) N^* Q k^2 - ab\lambda^2 \sin^2(\lambda x) N^* R k p_{im} \\ & + a\lambda \sin(\lambda x) N^* P k p_{im} \},\end{aligned}$$

$$\begin{aligned}(\psi_3)_4 = {} & M^* (p_1)_1 \{ k N^* (b\lambda \sin(\lambda x) - a\lambda \sin(\lambda x)) \\ & + \mu_T (k(R + Qb\lambda \sin(\lambda x)) \\ & + p_{im}(-Rb\lambda \sin(\lambda x) + P)) \},\end{aligned}$$

$$(\psi_4)_4 = -k N^* a\lambda \sin(\lambda x) p_{re} \mu_T (-Rb\lambda \sin(\lambda x) + P),$$

$$(\psi_1)_5 = (p_1)_1 (p_{re})_1 M^* \mu_T (-Rb\lambda \sin(\lambda x) + P),$$

$$\begin{aligned}(\psi_2)_5 = {} & (M^*)^2 (p_1)_1^2 + a\lambda \sin(\lambda x) N^* k \{ -kb\lambda \sin(\lambda x) N^* \\ & + kR\mu_T + kb\lambda \sin(\lambda x) Q \mu_T \\ & + \mu_T \left(P (p_{im})_1 - b\lambda \sin(\lambda x) R (p_{im})_r\right) \},\end{aligned}$$

$$\begin{aligned}(\psi_3)_5 = {} & M^* (p_1)_1 \{ k N^* (b\lambda \sin(\lambda x) - a\lambda \sin(\lambda x)) \\ & + \mu_T (k(R + Qb\lambda \sin(\lambda x)) \\ & + (p_{im})_1 (-Rb\lambda \sin(\lambda x) + P)) \}\end{aligned}$$

$$(\psi_4)_5 = -k N^* a\lambda \sin(\lambda x) (p_{re})_1 \mu_T (-Rb\lambda \sin(\lambda x) + P),$$

$$(\psi_1)_6 = (p_1)_2(p_{re})_1\mu_1\mu_T(-Rb\lambda\sin(\lambda x) + P),$$
$$(\psi_2)_6 = \mu_1^2(p_1)_2^2 + a\lambda\sin(\lambda x)$$
$$\mu_1 k\{(-kb\lambda\sin(\lambda x)\mu_1 + R\mu_T k + kb\lambda\sin(\lambda x)Q\mu_T)$$
$$+ \mu_T\big(P(p_{im})_1 - b\lambda\sin(\lambda x)R(p_{im})_1\big)\},$$
$$(\psi_3)_6 = \mu_1(p_1)_2\{k\mu_1(b\lambda\sin(\lambda x) - a\lambda\sin(\lambda x))$$
$$+ \mu_T(k(R + Qb\lambda\sin(\lambda x)) +.$$
$$+ (p_{im})_1(-Rb\lambda\sin(\lambda x) + P))\},$$
$$(\psi_4)_6 = -k\mu_1 a\lambda\sin(\lambda x)(p_{re})_1\mu_T(-Rb\lambda\sin(\lambda x) + P),$$

$$(p_1)_1 = k\sqrt{\left(\frac{c^2}{\beta_1^2} - \frac{N^*}{M^*}\right)},$$

$$(p_1)_2 = k\sqrt{\left(\frac{c^2}{\beta_1^2} - 1\right)},$$

$$(p_{im})_1 = \frac{1}{2}\frac{Rk}{P}, (p_{re})_1 = \frac{k}{2}\sqrt{4\left(\frac{Q - c^2/\beta_2^2}{P}\right) - \left(\frac{R}{P}\right)^2}.$$

References

1. Singh AK, Kumar S, Chattopadhyay A (2014) Effect of smooth moving punch in an initially stressed monoclinic magnetoelastic crystalline medium due to shear wave propagation. J Vib Control. doi:10.1177/1077546314549588
2. Singh AK, Das A, Chattopadhyay A, Dhua S (2015) Dispersion of shear wave propagating in vertically heterogeneous double layers overlying an initially stressed isotropic half-space. Soil Dyn Earthq Eng 69:16–27
3. Kumar R, Kumar R (2011) Analysis of wave motion at the boundary surface of orthotropic thermoelastic material with voids and isotropic elastic half-space. J Eng Phys Thermophys 84(2):463–478
4. Kundu S, Gupta S, Manna S (2014) SH-type wave dispersion in an isotropic medium sandwiched between an initially stressed orthotropic and heterogeneous semi-infinite media. Meccanica 49(3):749–758
5. Destrade M (2001) Surface waves in orthotropic incompressible materials. J Acoust Soc Am 110(2):837–840
6. Chow TS (1971) On the propagation of flexural waves in an orthotropic laminated plate and its response to an impulsive load. J Compos Mater 5(3):306–319
7. Prosser WH, Green RE (1990) Characterization of the nonlinear elastic properties of graphite/epoxy composites using ultrasound. J Reinf Plast Compos 9(2):162–173
8. Vinh PC, Seriani G (2010) Explicit secular equations of Stoneley waves in a non-homogeneous orthotropic elastic medium under the influence of gravity. Appl Math Comput 215(10):3515–3525
9. Spencer AJM (1972) Deformations of fibre-reinforced materials. Oxford University Press, New York
10. Belfield AJ, Rogers TG, Spencer AJM (1983) Stress in elastic plates reinforced by fibres lying in concentric circles. J Mech Phys Solids 31(1):25–54
11. Chattopadhyay A, Choudhury S (1995) Magnetoelastic shear waves in an infinite self-reinforced plate. Int J Numer Anal Meth Geomech 19(4):289–304
12. Chattopadhyay A, Singh AK (2012) Propagation of magnetoelastic shear waves in an irregular self-reinforced layer. J Eng Math 75:139–155
13. Chattopadhyay A, Singh AK (2013) Propagation of a crack due to magnetoelastic shear waves in a self-reinforced medium. J Vib Control 20(3):406–420
14. Chattopadhyay A, Singh AK (2012) G-type seismic waves in fibre reinforced media. Meccanica 47:1775–1785
15. Chattopadhyay A, Gupta S, Singh AK (2010) The dispersion of shear wave in multi-layered magnetoelastic self-reinforced media. Int J Solids Struct 47(9):1317–1324
16. Chattopadhyay A, Gupta S, Sahu SA, Singh AK (2013) Dispersion of horizontally polarized shear waves in an irregular non-homogeneous self-reinforced crustal layer over a semi-infinite self-reinforced medium. J Vib Control 19(1):109–119
17. Acharya DP, Roy I, Sengupta S (2009) Effect of magnetic field and initial stress on the propagation of interface waves in transversely isotropic perfectly conducting media. Acta Mech 202:35–45
18. Singh B, Yadav AK (2013) Reflection of plane waves in an initially stressed perfectly conducting transversely isotropic solid half-space. J Earth Syst Sci 122(4):1045–1053
19. Singh SS, Tomar SK (2008) qP-wave at a corrugated interface between two dissimilar pre-stressed elastic half-spaces. J Sound Vib 317(3):687–708
20. Kaur J, Tomar SK, Kaushik VP (2005) Reflection and refraction of SH-waves at a corrugated interface between two laterally and vertically heterogeneous viscoelastic solid half-spaces. Int J Solids Struct 42(13):3621–3643
21. Tomar SK, Kaur J (2003) Reflection and transmission of SH-waves at a corrugated interface between two laterally and vertically heterogeneous anisotropic elastic solid half-spaces. Earth Planets Space 55(9):531–547
22. Tomar SK, Kaur J (2007) SH-waves at a corrugated interface between a dry sandy half-space and an anisotropic elastic half-space. Acta Mech 190(1–4):1–28
23. Kaur J, Tomar SK (2004) Reflection and refraction of SH-waves at a corrugated interface between two monoclinic elastic half-spaces. Int J Numer Anal Meth Geomech 28(15):1543–1575
24. Kundu S, Manna S, Gupta S (2014) Love wave dispersion in pre-stressed homogeneous medium over a porous half-space with irregular boundary surfaces. Int J Solids Struct 51(21–22):3689–3697
25. Singh SS (2011) Love wave at a layer medium bounded by irregular boundary surfaces. J Vib Control 17(5):789–795
26. Ben-Hador R, Buchen P (1999) Love and Rayleigh waves in non-uniform media. Geophys J Int 137:521–534
27. Singh AK, Kumar S, Chattopadhyay A (2014) Effect of irregularity and heterogeneity on the stresses produced due to a normal moving load on a rough monoclinic half-space. Meccanica 49(12):2861–2878

28. Asano S (1966) Reflection and refraction of elastic waves at a corrugated interface. Bull Seismol Soc Am 56(1):201–221
29. Biot MA (1965) Mechanics of incremental deformations. Wiley, New York
30. Ewing WM, Jardetzky WS, Press F (1957) Elastic waves in layered media. McGraw-Hill, New York
31. Markham MF (1970) Measurements of elastic constants of fibre composites by ultrasonics. Composite 1:145–149
32. Gubbins D (1990) Seismology and plate tectonics. Cambridge University Press, Cambridge